Advancement in the understanding of multifragmentation and phase transition for hot nuclei

Bernard Borderie, Eric Bonnet, F. Gulminelli, N. Le Neindre, D. Mercier, S. Piantelli, Ad. R. Raduta, M. F. Rivet

Advancement in the understanding of multifragmentation and phase transition for hot nuclei

B. Borderie[1], E. Bonnet[1,2], F. Gulminelli[3], N. Le Neindre[1,3], D. Mercier[3,4], S. Piantelli[5], Ad. R. Raduta[6] and M. F. Rivet[1] for the INDRA and ALADIN collaborations

[1]Institut de Physique Nucléaire, CNRS/IN2P3, Univ. Paris-Sud 11, Orsay, France
[2]GANIL, DSM-CEA/CNRS-IN2P3,Caen, France
[3]LPC Caen, CNRS/IN2P3, ENSICAEN, Univ. de Caen, Caen, France
[4]Institut de Physique Nucléaire, IN2P3-CNRS et Université Lyon I, Villeurbanne, France
[5]Sezione INFN, Sesto Fiorentino (Fi), Italy
[6]National Institute for Physics and Nuclear Engineering, Bucharest-Măgurele, Romania

Abstract

Recent advancement on the knowledge of multifragmentation and phase transition for hot nuclei is reported. It concerns i) the influence of radial collective energy on fragment partitions and the derivation of general properties of partitions in presence of such a collective energy, ii) a better knowledge of freeze-out properties obtained by means of a simulation based on all the available experimental information and iii) the quantitative study of the bimodal behaviour of the heaviest fragment charge distribution for fragmenting hot heavy quasi-projectiles which allows, for the first time, to estimate the latent heat of the phase transition.

1 Introduction

Nucleus-nucleus collisions at intermediate energies offer various possibilities to produce hot nuclei which undergo a break-up into smaller pieces, which is called multifragmentation. The measured fragment properties are expected to reveal the existence on a phase transition for hot nuclei which was earlier theoretically predicted for nuclear matter [1, 2, 3]. By comparing in detail the properties of fragments ($Z \geq 5$) emitted by hot nuclei formed in central (quasi-fused systems, QF, from $^{129}Xe+^{nat}Sn$, 25-50 AMeV) and semi-peripheral collisions (quasi-projectiles, QP, from $^{197}Au+^{197}Au$, 80 and 100 AMeV), i.e. with different dynamical conditions for their formation, the role of radial collective energy on partitions is emphasized [4] and general properties of partitions are deduced (section 2). Then, in section 3, freeze-out properties of multifragmentation events produced in central collisions ($^{129}Xe+^{nat}Sn$) are estimated [5] and confirm the existence of a limiting excitation energy for fragments around 3.0-3.5 MeV per nucleon. The deduced freeze-out volumes are used as a calibration to calculate freeze-out volumes for QP sources; thus one can locate where the different sources break in the phase diagram. Finally, in section 4, the charge distribution of the heaviest fragment detected in the decay of QP sources is observed to be bimodal. This feature is expected as a generic signal of phase transition in nonextensive systems such as finite systems. For the first time an estimate of the latent heat of the transition is also extracted [6].

2 Radial collective energy and fragment partitions

To make a meaningful comparison of fragment properties which can be related to the phase diagram, hot nuclei showing, to a certain extent, statistical emission features must be selected. For central collisions (QF events) one selects complete and compact events in velocity space (constraint of flow angle $\geq 60°$). For peripheral collisions (QP subevents) the selection method applied to quasi-projectiles minimizes the contribution of dynamical emissions by imposing a compacity of fragments in velocity space. The excitation energies of the different hot nuclei produced are calculated using the calorimetry procedure (see [4] for details). By comparing the properties of selected sources on the same excitation energy domain, significant differences are observed above 5 AMeV excitation energy. QF sources have larger mean fragment multiplicities, $< M_{frag} >$, even normalized to the sizes of the sources (which differ by about 20% for QF and QP sources), and lower

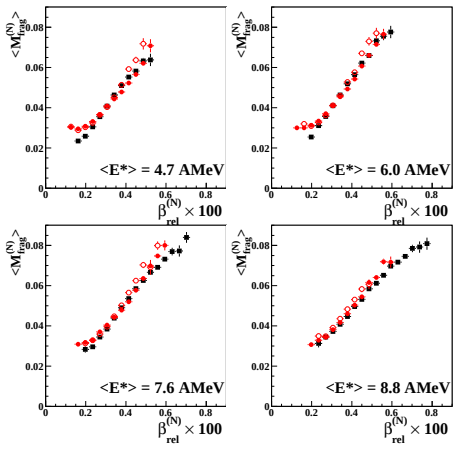

Figure 1: Evolution of the average fragment multiplicity normalized to the source charge/size $< M_{frag}^{(N)} >= < M_{frag}/Z_s >$ as a function of the relative velocity of fragments, β_{rel}^{N}, (see text) for different total excitation energy per nucleon of the sources.Full squares, open and full circles stand respectively for QF sources and QP sources produced at 80 and 100 MeV/nucleon incident energies.

values for generalized asymmetry: $A_Z = \sigma_Z/(\langle Z\rangle\sqrt{M_{frag}-1})$. A possible explanation of those different fragment partitions is related to the different dynamical constraints applied to the hot nuclei produced: a compression-expansion cycle for central collisions and a more gentle friction-abrasion process for peripheral ones.

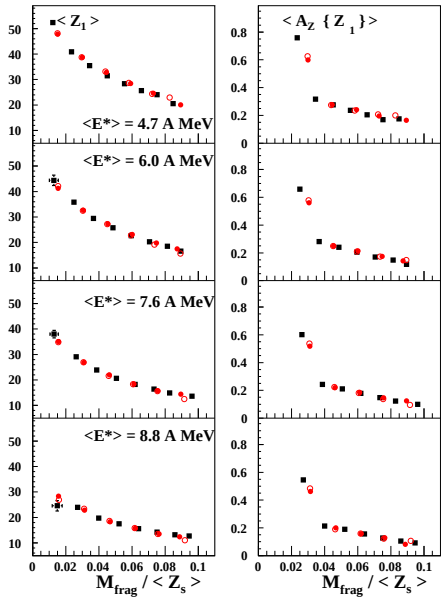

Figure 2: Left and right sides refer respectively to the mean charge of the heaviest fragment of partitions, $< Z_1 >$, and to the generalized asymmetry in charge of the fragment partitions without the heaviest one, $A_Z\backslash\{Z_1\}$, (see text) as a function of the reduced fragment mutiplicity, $M_{frag}/< Z_s >$, for different total excitation energy per nucleon of the sources.Full squares, open and full circles stand respectively for QF sources and QP sources produced at 80 and 100 MeV/nucleon incident energies.

The occurence of radial collective energy following a compression phase is predicted in semi-classical simulations of central collisions in the Fermi energy domain [7, 8]. In experiments it was recognized, in most of the

cases, from comparisons of kinetic properties of fragments with models. The mean relative velocity between fragments, β_{rel}, independent of the reference frame, allows to compare radial collective energy for both types of sources (QF or QP). The effect of the source size (Coulomb contribution on fragment velocities) can be removed by using a simple normalization which takes into account, event by event, the Coulomb influence, in velocity space, of the mean fragment charge, $\langle Z \rangle$, on the complement of the source charge $(Z_s - \langle Z \rangle)$: $\beta_{rel}^{(N)} = \beta_{rel}/\sqrt{\langle Z \rangle (Z_s - \langle Z \rangle)}$. At an excitation energy of about 5 AMeV, the $\beta_{rel}^{(N)}$ values corresponding to QF and QP sources are similar. Above that excitation energy, values for QF sources exhibit a strong linear increase, whreras for QP sources $\beta_{rel}^{(N)}$ only slightly increases up to 9-10 AMeV. That fast divergence between the values of $\beta_{rel}^{(N)}$ for the two types of sources signals the well known onset of radial collective expansion for central collisions. In [9], estimates of radial collective energy (from 0.5 to 2.2 AMeV) for QF sources produced by Xe+Sn collisions are reported for four incident energies: 32, 39, 45 and 50 AMeV. Those estimates which were extracted from comparisons with the statistical model SMM assuming a self similar expansion energy have been used to calibrate the $\beta_{rel}^{(N)}$ observable (see [4] for details). Then, one can show that radial collective energy is essentially due to thermal pressure for QP sources in semi-peripheral heavy-ion collisions as it is in hadron-induced reactions [10]. For QF sources produced in central heavy-ion collisions the contribution from the compression-expansion cycle becomes more and more important as the incident energy increases. Figure 1 shows, for different total excitation energy per nucleon corresponding to values defined by QF sources, the evolution of the average fragment multiplicity normalized to the source charge/size $< M_{frag}^{(N)} >= < M_{frag}/Z_s >$ as a function of β_{rel}^{N}. We observe a well defined correlation which fully confirms the role of collective energy in producing more fragments. Depending on the source type the relative contributions to radial collective energy of thermal pressure and cycle compression-expansion strongly differ [4] but anyhow β_{rel}^{N}, representative of the total collective energy, fixes the average degree of fragmentation (normalized mean fragment multiplicities).

Does the intensity of the radial collective energy also govern the details of fragment partitions, namely the relative charge/size of fragments in partitions. One can first consider the evolution of the size of the heaviest fragment, for given total excitation energies, with the reduced fragment multiplicities $M_{frag}/< Z_s >$. On the left panel of fig. 2 average values of the heaviest fragment charge for QP and QF sources are reported: they follow exactly the same evolution. Finally the division of the charge among

other fragments is investigated using the generalized asymmetry in charge of the fragment partitions. One can re-calculate the generalized asymmetry by removing Z_1 from partitions, noted $A_Z\backslash\{Z_1\}$. The results, displayed in fig. 2 (right panel) do not depend on the source type at a given total excitation energy and a given reduced fragment multiplicity. Note that the general asymmetry follows a linear trend except the lower reduced fragment multiplicity which corresponds to M_{frag}=2; indeed in that case, after removing Z_1, only one fragment is available for the asymmetry calculation and in each event the heaviest Z of the partition below Z equal 5 was taken. Such a result shows the subtle role played by the radial collective energy. It influences the overall degree of fragmentation but it does not affect the relative size of fragments in partitions for fixed reduced fragment multiplicities. Those results represent a benchmark against which models describing fragmentation of finite systems should be tested.

3 Freeze-out properties

Starting from all the available experimental information of selected QF sources produced in central ^{129}Xe+^{nat}Sn collisions which undergo multifragmentation, a simulation was performed to reconstruct freeze-out properties event by event [11, 5]. The method requires data with a very high degree of completeness, which is crucial for a good estimate of Coulomb energy. The parameters of the simulation were fixed in a consistent way including experimental partitions, kinetic properties and the related calorimetry. The necessity of introducing a limiting temperature related to the vanishing of level density for fragments [12] in the simulation was confirmed for all incident energies. This naturally leads to a limitation of their excitation energy around 3.0-3.5 AMeV as observed in [13]. The agreement between experimental and simulated velocity spectra for fragments of given charges (Z=6, 11, 18 and 27), for the different beam energies, is quite remarkable (see [5]). Finally relative velocities between fragment pairs were also compared through reduced relative velocity correlation functions [14, 15, 16, 17] (see fig. 3). In the simulation the fragment emission time is by definition equal to zero and correlation functions are consequently only sensitive to the spatial arrangement of fragments at break-up and the radial collective energy involved (hole at low reduced relative velocity), to source sizes/charges and to excitation energy of the sources (more or less pronounced bump at v_{red}= 0.02-0.03c). Again a reasonable agreement is obtained between experimental data and simulations, especially at 39 and 45 AMeV incident energies,

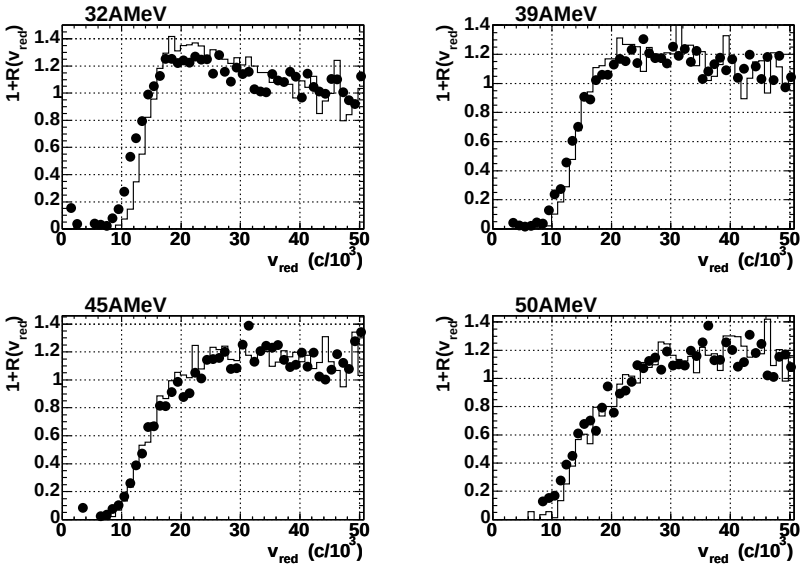

Figure 3: Comparison between the experimental (full points) and simulated (histograms) reduced relative velocity correlation functions for all the fragments. The reduced relative velocity between two fragments with charges Z_i and Z_j ($Z_{i,j}$ >4) is defined as v_{red}=$v_{rel}/(Z_i + Z_j)^{1/2}$. Each panel refers to a different beam energy: 32 AMeV (top left), 39 AMeV (top right), 45 AMeV (bottom left) and 50 AMeV (bottom right). From [5].

which indicates that the retained method and parameters are sufficiently relevant to correctly describe freeze-out topologies and properties.

The major properties of the freeze-out configurations thus derived are the following: an important increase, from ∼20% to ∼60%, of the percentage of particles present at freeze-out between 32 and 45-50 AMeV incident energies accompanied by a weak increase of the freeze-out volume which tends to saturate at high excitation energy. Finally, to check the overall physical coherence of the developed approach, a detailed comparison with a microcanonical statistical model (MMM) was done. The degree of agreement, which was found acceptable, confirms the main results and gives confidence in using those reconstructed freeze-out events for further studies as it is done in [4]. Estimates of freeze-out volumes for QF sources produced in Xe+Sn collisions for incident energies between 32 and 50 AMeV evolve from 3.9 to 5.7 V/V_0, where V_0 would correspond to the volume of the source at normal density [5].

To calibrate the freeze-out volumes for other sources, we use the charge of the heaviest fragment $< Z_1^{(N)} >$ or the fragment multiplicity $< M_{frag}^{(N)} >$, normalized to the size of the source, as representative of the volume or density at break-up. From the four points for QF sources and the additional constraint that $Z_1^{(N)} = M_{frag}$=1 at V/V_0=1, we obtain two relations $V/V_0 = f_1(Z_1^{(N)})$ and $V/V_0 = f_2(M_{frag}^{(N)})$, from which we calculate the volumes for QF sources at 25 AMeV and for QP sources. The results are plotted in fig. 4, with error bars coming from the difference between the two estimates using f_1 and f_2; note that error bars for the QP volumes are small up to 7 AMeV, and can not be estimated above, due to the fall of $< M_{frag}^{(N)} >$ at high energy (see fig. 5 of [4]). So only $< (Z_1^{(N)} >)$ can be used over the whole excitation energy range considered and the derived function is the following:
$V/V_0 = exp(2.47 - 4.47 < (Z_1^{(N)} >) + 0.86$.

The volumes of QP sources are smaller than those of QF sources (by about 20% on the E^* range 5-10 AMeV).

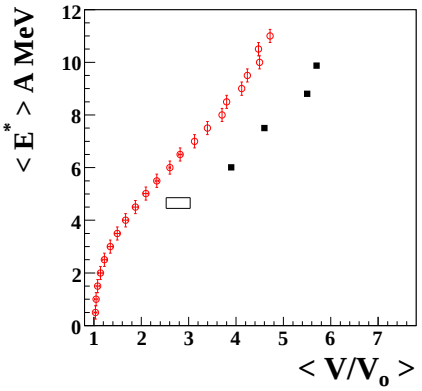

Figure 4: Fragmentation position in the excitation energy-freeze-out volume plane. The four full squares (QF sources) are taken from [5]. The open rectangle gives the estimated position (with error bar) for QF source at 25 AMeV, and the open circles those for QP sources. From [4].

Z_1 also presents some specific dynamical properties. As shown in [18, 17] for QF sources, its average kinetic energy is smaller than that of other fragments with the same charge. The effect was observed whatever the fragment multiplicity for Xe+Sn between 32 and 50 AMeV and for Gd+U at 36 AMeV. The fragment-fragment correlation functions are also different when one of the two fragments is Z_1. This observation was connected to the event topology at freeze-out, the heavier fragments being systematically closer to the centre of mass than the others.

4 Bimodality of the heaviest fragment and latent heat of the transition

At a first-order phase transition, the distribution of the order parameter in a finite system presents a characteristic bimodal behaviour in the canonical or grandcanonical ensemble [19]. The bimodality comes from an anomalous convexity of the underlying microcanonical entropy [20]. It physically corresponds to the simultaneous presence of two different classes of physical states for the same value of the control parameter, and can survive at the thermodynamic limit in a large class of physical systems subject to long-range interactions [21]. In the case of hot nuclei which undergo multifragmentation, the size/charge of the heaviest fragment was early recognized as an order parameter [22, 23] using the universal fluctuation theory. In a quantitative analysis for QP sources, the robustness of the signal of bimodality is tested against two different QP selection methods [6]. A weighting procedure [24] is used to test the independence of the decay from the dynamics of the entrance channel and to allow a comparison with canonical expectations. Finally, a double saddle-point approximation is applied to extract from the measured data an equivalent-canonical distribution. To take into account the small variations of the source size, the charge of the heaviest fragment Z_1 has been normalized to the source size. After the weighting procedure, a bimodal behaviour of the largest fragment charge distribution is observed for both selection methods. Those weighted experimental distributions can be fitted with an analytic function (see [6] for more details). From the obtained parameter values one can estimate the latent heat of the transition of the hot heavy nuclei studied (Z$\sim$70) as $\Delta E = 8.1(\pm 0.4)_{stat}(+1.2 - 0.9)_{syst}$ AMeV. Statistical error was derived from experimental statistics and systematic er-

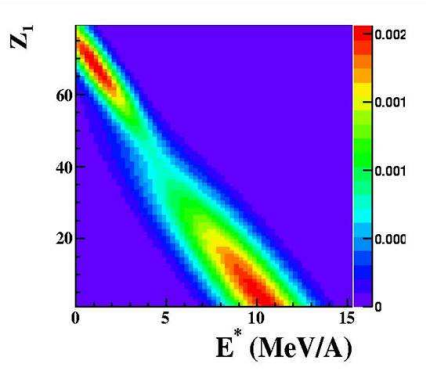

Figure 5: Size of the heaviest fragment versus total excitation energy in AMeV. That picture is constructed using the fit parameters extracted from the equivalent-canonical distribution. The distance between the two maxima, liquid and gas peaks, projected on the excitation energy axis corresponds to the latent heat of the transition.

rors from the comparison between the different QP selections. The results (for one QP source selection) are illustrated in fig. 5. A detailed presentation and discussion of those results is also found in [25].

5 Conclusion

Today a rather coherent and complete picture has been reached for a few exhaustive studies concerning multifragmentation and the related liquid-gas type phase transition which occurs at excitation energies between 2-3 and 9-10 AMeV. Only the mechanism of fragment formation is still an open question: spinodal fluctuations in stochastic mean field approaches or many-body correlations early built in molecular dynamics [3]. At present, with the introduction of the N/Z degree of freedom in such studies, new signals predicted by theory must be investigated to precise and strengthen our actual knowledge. It concerns fractionation (liquid more symmetric due to minimization of symmetry energy in dense phase), increased fractionation if spinodal instabilities are responsible for fragment formation, and the reduction of spinodal zone for large N/Z values involved. For the future the introduction of the N/Z degree of freedom will permit to improve fundamental information on the phase diagram of baryonic matter. Moreover hot exotic nuclei appear as a unique laboratory to serve as test-bench for theory of phase transitions of finite quantum systems with two components.

References

[1] B. Borderie, *J. Phys. G: Nucl. Part. Phys.* **28** (2002) R217.

[2] P. Chomaz, F. Gulminelli et al. (eds.) vol. 30 of *Eur. Phys. J. A*, Springer, 2006.

[3] B. Borderie and M. F. Rivet, *Prog. Part. Nucl. Phys.* **61** (2008) 551.

[4] E. Bonnet, B. Borderie et al. (INDRA and ALADIN Collaborations), *Nucl. Phys.* **A 816** (2009) 1.

[5] S. Piantelli, B. Borderie et al. (INDRA Collaboration), *Nucl. Phys.* **A 809** (2008) 111.

[6] E.Bonnet, D. Mercier et al. (INDRA Collaboration), *Phys. Rev. Lett.* **103** (2009) 072701.

[7] J. J. Molitoris, A. Bonasera et al., *Phys. Rev.* **C 37** (1988) 1020.

[8] E. Suraud, M. Pi et al., *Phys. Lett.* **B 229** (1989) 359.

[9] G. Tăbăcaru, B. Borderie et al., *Eur. Phys. J.* **A 18** (2003) 103.

[10] L. Beaulieu, T. Lefort et al., *Phys. Rev. C* **64** (2001) 064604.

[11] S. Piantelli, N. Le Neindre et al. (INDRA Collaboration), *Phys. Lett.* **B 627** (2005) 18.

[12] S. E. Koonin and J. Randrup, *Nucl. Phys.* **A 474** (1987) 173.

[13] S. Hudan, A. Chbihi et al. (INDRA Collaboration), *Phys. Rev.* **C 67** (2003) 064613.

[14] Y. D. Kim, R. T. de Souza et al., *Phys. Rev.* **C 45** (1992) 338.

[15] D. R. Bowman, N. Colonna et al., *Phys. Rev.* **C 52** (1995) 818.

[16] D. H. E. Gross, *Phys. Rep.* **279** (1997) 119.

[17] G. Tăbăcaru, M. F. Rivet et al. (INDRA Collaboration), *Nucl. Phys.* **A 764** (2006) 371.

[18] N. Marie, R. Laforest et al. (INDRA Collaboration), *Phys. Lett.* **B 391** (1997) 15.

[19] F. Gulminelli, *Ann. Phys. Fr.* **29** (2004) N^o 6.

[20] D. H. E. Gross, Microcanonical thermodynamics, World Scientific, 2002, vol. 66 of *World scientific Lecture Notes in Physics*.

[21] T. Dauxois et al. (eds.) vol. 602 of *Lecture Notes in Physics*, Springer-Verlag, Heidelberg, 2002.

[22] R. Botet, M. Płoszajczak et al., *Phys. Rev. Lett.* **86** (2001) 3514.

[23] J. D. Frankland, A. Chbihi et al. (INDRA and ALADIN collaborations), *Phys. Rev.* **C 71** (2005) 034607.

[24] F. Gulminelli, *Nucl. Phys.* **A 791** (2007) 165.

[25] E. Bonnet, this workshop.